Bulletin of Electrical Engineering and Informatics
Vol. 13, No. 6, December 2024, pp. 4168~4181
ISSN: 2302-9285, DOI: 10.11591/eei.v13i6.8120

Multispectral imaging and deep learning for oil palm fruit bunch ripeness detection

Minarni Shiddiq[1], Saktioto[1], Roni Salambue[2], Fiqra Wardana[2], Vicky Vernando Dasta[1], Ihsan Okta Harmailil[1], Mohammad Fisal Rabin[1], Nisa Arpyanti[1], Dilham Wahyudi[1]
[1]Department of Physics, Faculty of Mathematics and Natural Sciences, University of Riau, Pekanbaru, Indonesia
[2]Department of Computer Science, Faculty of Mathematics and Natural Sciences, University of Riau, Pekanbaru, Indonesia

Article Info

Article history:

Received Dec 29, 2023
Revised Jun 7, 2024
Accepted Jun 26, 2024

Keywords:

Deep learning
Light-emitting diode array
Multispectral imaging
Oil palm fresh fruit bunches
Ripeness detection
You only look once version 4

ABSTRACT

Oil palm fresh fruit bunches (FFBs) are the raw material of crude palm oil (CPO) on which ripeness levels of FFBs are essential to obtain good quality CPO. Most palm oil mills use experienced graders to evaluate FFB ripeness levels. Researchers have developed rapid and non-destructive methods for ripeness detection using computer vision (CV) and deep learning. However, most of the experiments used color cameras, such as a webcam or a smartphone, limited to visible wavelengths, and used still FFBs on–trees or on the ground. This study developed a light-emitting diode (LED)-based multispectral imaging system with deep learning for rapid and real-time ripeness detection of oil palm FFBs on a moving conveyor. The ripeness levels used were unripe and ripe. We also evaluated the spectrum of reflectance intensities for the ripeness levels. The ripeness detection system employed a two-class you only look once version 4 (YOLOv4) detection model using a dataset of 2000 annotated unripe and ripe FFB multispectral images and a video of 30 moving FFBs for real-time testing. The results show a promising method to detect oil palm FFB ripeness with an average accuracy of 99.66% and a speed range of 3.32-3.62 frame per second (FPS).

Corresponding Author:

Minarni Shiddiq
Department of Physics, Faculty of Mathematics and Natural Sciences, University of Riau
28293 Pekanbaru, Riau, Indonesia
Email: minarni.shiddiq@lecturer.unri.ac.id

1. INTRODUCTION

Imaging methods have been developed and applied intensively in agriculture for fruit and vegetable quality assessments for the last decades. The fruit and vegetable assessment activities include maturity or ripeness detection, fruit counting, and storage life estimation. The methods can evaluate the external or internal qualities of fruits and vegetables. Maturity and ripeness stages are important fruit qualities that need monitoring and detection. Many efforts have explored innovative imaging technologies for fast, reliable, real-time, and non-destructive methods to detect fruit and vegetable ripeness stages [1]. The imaging techniques fall into three main categories: vision-based, spectroscopic, and mechanical methods [2]. The vision-based method is computer vision (CV), which includes color imaging, hyperspectral, and multispectral imaging. Color imaging refers to the visible region red, green, blue (RGB) imaging. It is simple and low-cost imaging but limited spectral resolution since only three wavelength bands are available. Most fruits and vegetables reflect light in infrared (IR) regions. Hyperspectral and multispectral imaging consist of many wavelength regions (ultraviolet, visible, IR) depending on how many bands are applied. Multispectral imaging uses fewer bands (less than 10 λ). Hyperspectral and multispectral imaging have flourished in applications due to their spatial and spectral resolution. It becomes an intelligent imaging method if accompanied by machine learning

or deep learning [3]. Hyperspectral and multispectral imaging have found applications in machine vision (MV). MV is a complete system that uses CV along with machine components to build an automatic system, such as a conveyor unit, motors, and separators, in addition to deep learning algorithms, such as artificial neural networks (ANN) and convolutional neural networks (CNN) [4].

Hyperspectral and multispectral imaging are also called spectral imaging as the combination of CV and spectroscopy. The imaging techniques find broad applications in agriculture, including post-harvest fruit quality evaluation based on ripeness levels and physicochemical parameters such as moisture content, dry matter content, and firmness [5]. Multispectral imaging has some practical advantages over hyperspectral imaging when applied to fruit sorting and grading, such as low cost, simplicity, and less image processing time due to fewer wavelength bands. Recently, multispectral systems using light-emitting diodes (LEDs) have become an acceptable, low-cost choice due to the availability of commercial narrow-bandwidth LEDs. The traditional multispectral imaging system uses commercial multispectral or monochrome cameras and a color filter array with halogen lamps as light sources, which are relatively expensive and complex experimental setups. In addition, the LED array has a faster switching time for changing wavelength light [6]. Multispectral imaging systems based on LED arrays have applications for detecting rice false smut (RFS) of two different cultivars of rice seeds [7] and human tongue health [8]. CV system is an efficient fruit grading or classification system if supported by appropriate machine learning algorithms, such as partial least square discriminant analysis (PLS-DA), multi-layer perceptron (MLP), and linear discriminant analysis (LDA) [9].

Spectral imaging with deep learning has been explored recently for two reasons: spectral imaging requires faster classification algorithms and the traditional object detection CV needs object spectral information. CV based on object detection method has gained many applications in fruit and vegetable classification due to the advancement of CNN series, such as faster region with CNN (R-CNN) and you only look once (YOLO). However, YOLO algorithms produce higher frame per second (FPS) than faster R-CNN [10]. Scanning using spectral imaging is prone to big spectral data, low image acquisition speed, and long image processing time. Spectral imaging with deep learning proposes fast reconstruction speed, quality, and less computational time [11]. Spectral imaging with object detection offers real-time, faster, and higher accuracy detection with fewer spectral images [12]. Some experiments have used deep learning based-spectral imaging, such as the developments of a region-free object detector named YOLO-FIRI for IR images with YOLOv5 algorithms [13] and a multispectral based object recognition system with YOLOv3 and YOLOv4 algorithms, for a well-organized dataset of outdoor scenes in three spectra: visible RGB, near-infrared (NIR), and thermal [14]. Another application of deep learning-based spectral imaging was an intelligent separation method for coal gangue based on multispectral imaging technology and object detection of YOLO v4.1 models [15].

Crude palm oil (CPO) is one of the export commodities for Indonesia and Malaysia. CPO quality and palm oil industry sustainability are crucial, and some efforts are essential to promote quality assurance and automation in palm oil industries. Oil palm fresh fruit bunches (FFBs) are the raw material of CPO. Sorting and grading FFBs is a principal step when FFBs arrive at the sorting facility of a palm oil mill. The sorting and grading process at the sorting area usually uses experienced workers who sort defective and unripe oil palm FFBs. Grading criteria are related to internal characteristics of oil palm FFBs, such as oil contents (OC) and free fatty acid (FFA). The chemical contents are associated with the ripeness stages of oil palm FFBs, on which ripe FFBs have maximum OC and acceptable FFA content [16]. Manual and traditional sorting and grading processes of oil palm FFBs are prone to damaged FFBs and inaccuracy due to subjectivity, plenty of laborers, and long work hours. Palm oil industry stakeholders are reluctant to embrace the new technology of the Industry 4.0 concept in the palm oil industry, especially at the plantations and palm oil refineries [17]. Experiments to obtain a real-time, fast, reliable, low-cost, non-destructive assessment system for oil palm FFBs have been continuous strides for decades. Many non-destructive methods have been developed, such as fluorescence imaging, NIR spectroscopy, thermal imaging, visible CV, and spectral imaging. The quality parameters evaluated are ripeness stages and the related physico-chemical parameters. Hyperspectral and multispectral imaging have found applications for the oil palm FFB ripeness classification [18]. Deep learning using YOLO algorithms also has applications in on-tree oil palm FFB ripeness detection during harvesting, such as using the YOLOv3 algorithm [19], an optimized YOLOv3 tiny (YOLO-P) [20], and YOLOv4 [21]. Ripeness detection and classification of on-the-ground oil palm FFBs have also used YOLO algorithms, such as YOLOv5 series and other deep learning algorithms [22], and modified YOLOv4 models [23].

This study used multispectral imaging and deep learning of the YOLO algorithm to detect the ripeness stages of oil palm FFBs on a moving conveyor. Most detection methods for oil palm ripeness levels used stationary oil palm FFBs on trees or on the ground. The cameras were attached to a drone or using a smartphone. The contributions of this study are as follows: i) CV with a USB camera and its driver enable integration to mechatronics of an automatic MV using the Python-based acquisition and processing program; ii) using YOLOv4 algorithms based on video frames allows the FFB ripeness detection without stopping the

conveyor, offering a rapid and real-time postharvest sorting and grading process. For this study, we used the ripeness levels as unripe and ripe and only a separator arm for practical reasons. Other ripeness levels can be easily included by adding more classes and their datasets in the detection model; iii) the imaging system used a donut-shaped LED array with eight wavelengths in visible and IR regions, which was a replacement for multispectral imaging based on halogen lamps and filter wheels; iv) the acquisition program allows each LED in the array to switch off or all LEDs turned on and record multispectral images simultaneously; and v) using a monochrome camera has the benefit of monochrome images, which are insensitive to background light compared to color cameras [14]. Monochrome camera sensors have higher quantum efficiency (QE) and sensitivity in visible and IR regions, unlike color cameras only in the visible region.

2. METHOD

The study has two experiments: analyzing ripeness levels of oil palm FFBs using reflectance intensities at different wavelengths and detecting the ripeness levels using a YOLO algorithm, as described in Figure 1. The first experiment aims to obtain the average reflectance intensity for each oil palm FFB based on its ripeness levels and the LED wavelengths. The numerical dataset can be analyzed afterward using principal component analysis (PCA) or, as the input of an ANN classification model or, partial least squares (PLS) [24]. The second experiment is to detect the ripeness levels of oil palm FFBs using multispectral images as the input of a YOLO model. The YOLO ripeness detection experiment has some stages, including image acquisition, annotation, dataset construction, model training, testing, and using the model to detect ripeness levels in a real-time scheme. All the stages used Python-based scripts. This study is the preliminary step toward applying IR multispectral images for oil palm FFB grading using the object detection algorithm. It is possible to reconstruct the images according to their wavelengths as spectral signatures using a wavelength-coded or with other properties of light involved, such as amplitude-coded and phase-coded methods [11]. The bounding box will have spatial and spectral resolution.

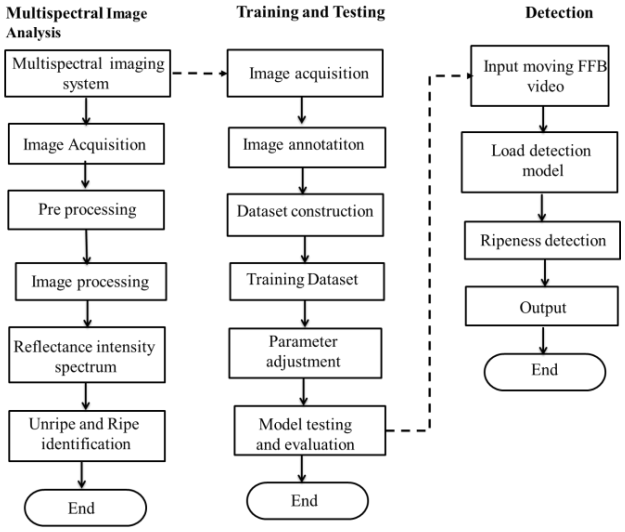

Figure 1. Research stages of oil palm FFB ripeness detection

2.1. Multispectral imaging system

The LED multispectral imaging system used in this study is part of a MV system for oil palm FFB, built in a previous experiment using a pair of halogen lamps and a filter wheel [24]. The main components of the MV system are shown in Figure 2. The system consists of a conveyor unit, an optical portal, a pneumatic-based separator, and a personal computer (PC). The conveyor type is a driven-chain conveyor, which moves oil palm FFBs to the optical portal. The portal contains a multispectral imaging unit and black metal shielding to block the background light from entering the camera. The box has frames and holders for the multispectral imaging unit components. It has entrances with black-cloth fringes on the left and right side to pass through an oil palm FFB. The system has an Arduino UNO board to connect a PC to the actuators and LED array. A proximity sensor is positioned before FFB enters the optical portal to initiate the image recording and processing.

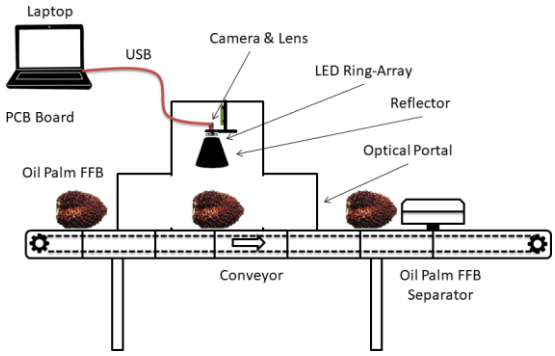

Figure 2. MV system for oil palm FFBs

The multispectral imaging unit shown in Figure 2 has some optical components, including an LED array and a camera with a lens. The camera was a Sentech NIR monochrome complementary metal–oxide–semiconductor (CMOS) camera with a resolution of 2.2 MP (2048×1088 pixels) and a sensor size of 2/3", 167 FPS, a Navitar lens of 12 mm F/1.4 1". The camera and LED array control use a 3.10.2 Python-based acquisition program. Other specifications for the camera are a USB connection, trigger, I/O inputs, and a compatible camera driver. The multispectral unit was installed at the middle-top optical portal with a 65 cm distance from the lens to the conveyor surface (about 35 cm working distance). The conveyor plate at the portal base has a black film to reduce reflection from the plate surface. The LED array uses eight well-defined bandwidth LEDs as light sources. The selected wavelengths were obtained previously using filter wheel-based multispectral imaging for oil palm FFBs [18].

Figure 3 shows the optical and electronic components of the LED-based multispectral imaging unit. Figure 3(a) shows the unit has three printed circuit boards (PCBs), control, Arduino, and LED circuit boards. The LED circuit board is attached to an acrylic plate, functioning as the unit stand. The acrylic has bored 1/4"-20 (M6) tapped holes to accommodate Thorlabs 1/2" optical posts. The optical posts help the unit attach to the upper middle of the optical portal with Thorlabs post holders and a 12×5-inch optical board posted to the inner top portal frame. The microcontroller and PCB board with a current divider control the currents through each LED and can turn each LED on and off accordingly. Figure 3(a) also shows an aluminum lamp cap used as the light reflector with 15 cm in diameter. It has a dome shape that helps to converge light from each LED to oil palm FFB. The LED array has 32 narrowband LEDs with eight wavelengths, which are 680, 700, 750, 780, 810, 850, 880, and 900 nm. The LEDs have 8-24 mW powers and 25-35 nm bandwidths. Each wavelength has 4 LEDs positioned at four corners in the doughnut-shaped array. Figure 3(b) shows a 680 nm LED lighted up at four corners.

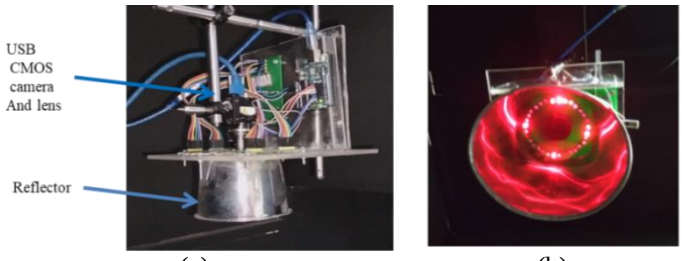

(a) (b)

Figure 3. Multispectral imaging unit based on LED array; (a) unit hardware and (b) 680 nm LED light

The samples were Tenera oil palm FFBs from two plantations, a government-owned and a smallholder plantation. The samples consisted of unripe and ripe oil palm FFBs. Each oil palm FFB has a label on its base according to the sample number and ripeness level. The ripeness levels of the samples get validated by certified graders of the plantations based on skin and mesocarp colors and loose fruit numbers from bunches. Figures 4(a) to (h) shows the color images of unripe and ripe oil palm FFB samples. The unripe FFBs colors are blackish-purplish, while the ripe colors range from reddish to orange. There is a different fruit density between the front and back sides of oil palm FFB, especially at the basal part. Oil palm

FFB ripeness can also be classified based on several loose fruits called fractions (F). Unripe FFBs include the fractions of F0 and F1 with red blackish, while ripe FFBs have F2 and F3 fractions with red yellowish. F4 fraction is overripe level but can be included as ripe FFBs in this experiment with the same color [25].

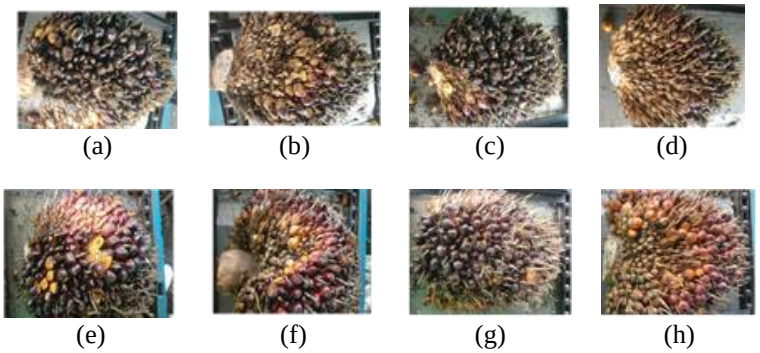

Figure 4. Oil palm FFB samples; (a) front unripe S1, (b) back unripe S1, (c) front unripe S2, (d) back unripe S2, (e) front ripe S1, (f) back ripe S1, (g) front ripe S2, and (h) back ripe S2

2.2. Multispectral image analysis

This study used two image acquisition schemes. The first scheme intends to obtain the reflectance intensity spectrum for each ripeness level, as described in Figure 4. The samples were 15 unripe and 15 ripe FFBs. The acquisition technique used single-shot multispectral imaging, which imitated the image acquisition stage of traditional multispectral imaging using an 8-wavelength filter wheel [18]. Here, we used eight LEDs with different wavelengths for multispectral imaging. In this scheme, the acquisition program recorded eight images for each oil palm FFB side, related to turning on and off each LED sequentially, and the camera recorded each image. The recording occurs when the FFB is placed at the center of the optical portal using the conveyor. After recording images of eight wavelengths on each side, the oil palm moved out of the portal. The acquisition stage resulted in 30 images for each ripeness level. White and dark reference images have been recorded and placed in the image processing database for calibration [24]. OC and FFA of each oil palm FFB were measured using the Soxhlet extraction method right after the image acquisition stage. Figure 5 shows the image processing flowchart.

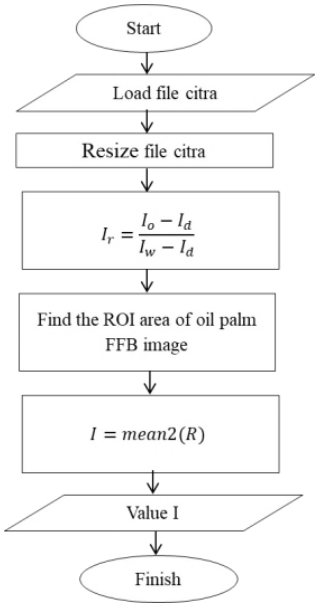

Figure 5. Multispectral image processing flowchart

The image processing for this scheme aims to obtain the relative intensity for each FFB at each wavelength. The acquisition step obtained 60 images, which consisted of 30 images for each ripeness level, corresponding to two FFB sides and 8 LED wavelengths. Figure 5 shows the image processing flowchart. The first step is to load and resize a recorded multispectral image into a size of (1024, 540) pixels. The multispectral image (Io) was then corrected using white reference (Iw) and black reference (Id) images to obtain a calibrated image (Ir). The white reference image is used as the reference reflectance intensity, while the black reference image eliminates the effect of dark currents from the sensitive detector. After image calibration, the ROI (region of interest) area is determined, which contains the FFB sample. In this case, the ROI was the (614,326) pixels in size. The average intensity calculation aims to obtain the FFB reflectance intensity at a particular wavelength and ripeness level.

2.3. Image acquisition for you only look once model

We have used multispectral images from some sources to build a dataset for ripeness YOLO model detection of oil palm FFBs. The first source was from the state-owned plantation, PTPN V, Pekanbaru, Riau. We brought the system to the sorting area of the plantation. The dataset consisted of 356 ripe and 176 unripe oil palm FFB multispectral images, including 30 FFBs used for reflectance intensity analysis. Two experienced graders validated each FFB ripeness level. The image acquisition setting for each oil palm FFB was with all LEDs light on. Each FFB was scanned twice at the front and back sides. We recorded two videos of moving 15 unripe and 15 ripe FFBs for the model validation. The imbalance of image quantities of ripe and unripe FFBs is due to the strict regulation in the sorting area, which makes it hard to find unripe FFBs. We added more multispectral images from previous experiments using filter-wheel-based multispectral imaging with the same classification, ripe and unripe oil palm FFBs. The experiment used oil palm FFBs from private or smallholder plantations. As a result, we have collected 2000 multispectral images using oil palm FFB samples from PTPN V and private plantations for the YOLO model, which consisted of 1000 unripe images and 1000 ripe images. The multispectral ripe FFB images had 356 images using the LED setup and 644 images using the previous halogen-based setup. In the meantime, the unripe TBS images had 176 images using the LED setup and 824 images using the halogen experiment [18], [24].

2.4. You only look once model construction

Before building a custom YOLO model, an annotation process is essential. Annotation is a labeling stage using a labeling tool that aims to prepare the detection program to identify objects in a set of still images or video frames, in this case, oil palm FFBs in two ripeness classes, unripe and ripe. The labeling gives a bounding box and class name on an object inside an image. One of the available labeling tools is the Python application program LabelImg, which results in a file in .txt format, which contains image data such as the bounding box size and class number. Its coordinate numbers specify the bounding box size. The file .txt has format as <object-class> <x_center><y_center> <width><height>. In this study, <object-class> was 0 for the ripe and 1 for the unripe class. The <x_center> and <y_center> coordinates represent the bounding box center, such as for ripe and unripe classes, respectively are (0.484568, 0.490741) and (0.510586, 0.452454). The values of <width> and <height> mean as normalized width or height of the object's bounding box relative to the width or height of the image, as examples here are (0.722222, 0.956790) and (0.688925, 0.898773).

Construction of the YOLO model for oil palm FFB ripeness detection used the annotated dataset of multispectral images obtained by acquisition and annotation processes. The multispectral images had the LED wavelengths the same as in the previous experiment, which used a filter wheel [18]. The ripeness detection model used the YOLOv4tiny algorithm. YOLOv4 algorithms have had many applications recently in fruit and vegetable sorting MV due to more accuracy and less processing time. YOLOv4 tiny was the ideal model for high speed and less computational time [26]. The YOLOv4 tiny configuration file for oil palm FFB ripeness detection has parameters including batch number, subdivisions, width, height, classes, and filters. The used parameters are generic from the darknet framework and adjusted through the training stage to obtain the best ripeness detection model. The YOLOv4 configuration file had 6000 steps or iterations, a batch number of 64, a subdivision of 16, a width of 416, a height of 416, classes of 2, and filters of 21.

2.5. Model training and testing

Training and testing are the crucial steps in constructing classification or detection models. The training aims to analyze the ripeness detection model, hence being able to recognize unripe and ripe oil palm FFBs from the annotated multispectral images. Dataset training has used the Google Colaboratory (Colab) platform and used pre-trained weight YOLOv4 tiny with fine-tuning. This study obtained 2000 annotated images for building the YOLO model, which consisted of 1.000 images for ripe and 1000 for unripe oil palm FFBs. The dataset was divided into training, testing, and validation subsets. Table 1 shows the dataset splits, comprising 1520 images for training, 380 images for testing, and 100 images for validation processes. So, the

total number of images for training and testing was 1900. We used 100 images for metrics analysis. Additional validation was performed using two separate 15 FFBs videos of ripe and unripe FFBs for real-time detection.

Table 1. Dataset splits for YOLO model training and testing

Name of split	Number
"ripe" in training	761
"unripe" in training	759
"ripe" in testing	190
"ripe" in testing	190
"ripe" in validation	49
"unripe" in validation	51

The YOLO model for oil palm FFB ripeness detection requires performance analysis or evaluation. In this study, model evaluation used confusion matrix and other statistical values. Confusion matrix forms a value matrix that compares predicted and actual values (ground truth) using four components: true positive (TP), false positive (FP), true negative (TN), and false negative (FN). We assigned positive or negative values to unripe and ripe FFB states for the ripeness detection model. Other parameters of the confusion matrix are recall, precision, and F1-score, obtained using (1) to (3), respectively. There are three other parameters often used for YOLO model performance analysis: average precision (AP), mean average precision (mAP), and intersection over union (IoU), calculated using (4) to (6), respectively. They are related to the confusion matrix's four components [27]. In this study, the computation of the performance parameters of a YOLO detection model uses the sci-kit-learn package of Python.

$$\text{Recall (R)} = \frac{\text{TP}}{\text{TP+FN}} \tag{1}$$

$$Precision\ (P) = \frac{TP}{TP+FP} \tag{2}$$

$$F1 - score = \frac{2\ x\ (\ Precision\ x\ Recall)}{Precision+Recall} \tag{3}$$

$$AP = \sum(Recall\ (n+1)\ -\ Recall\ (n))\ x\ Precision\ x\ Recall\ (n+1) \tag{4}$$

$$mAP = \frac{1}{n} \sum_{k=1}^{k=n} AP(k) \tag{5}$$

$$IoU = \frac{area\ of\ overlap}{area\ of\ union} \tag{6}$$

3. RESULTS AND DISCUSSION

This study aimed to use LED-based multispectral imaging and YOLOv4 tiny models to detect unripe and ripe oil palm FFBs on a moving conveyor. The unit is part of a MV system for sorting and grading oil palm FFBs. Annotated images of still oil palm FFBs on the conveyor were used for model training and streaming videos of moving oil palm FFBs for real-time testing. The testing results show that each detected oil palm bunch image displays a bounding box, ripeness classification, and accuracy value. The fine-tuning step of the YOLOv4 tiny model was performed using configuration files on the cloud Google Colab Pro Platform. The configuration file contains model parameters and pre-trained weights of previously trained YOLO models.

3.1. Multispectral images

We used 30 oil palm FFBs to show the characteristics of oil palm FFBs ripeness stages in terms of relative reflectance intensities and chemical contents of the oil palm FFBs. The multispectral images were acquired at different wavelengths. Each FFB has a stack of monochrome images at LED wavelengths of 680 nm, 700 nm, 750 nm, 780 nm, 810 nm, 850 nm, 880 nm, and 900 nm, as shown in Figures 6(a) and (b). The obtained monochrome images consisted of 2 ripeness levels, and each FFB has front and back side images. As shown in Figure 4, the RGB colors of unripe FFBs are darker than ripe FFBs, consistent with Figure 6, having lower intensities. The ripe fruits of oil palm FFBs reflect more light than the unripe fruits.

Unripe fruits have more chlorophyll and anthocyanin contents, which absorb more light in the visible region [28]. Figure 6 also shows increasingly less visible images as the wavelengths increase in the IR region, invisible to the human eye but sensible by the NIR monochrome camera.

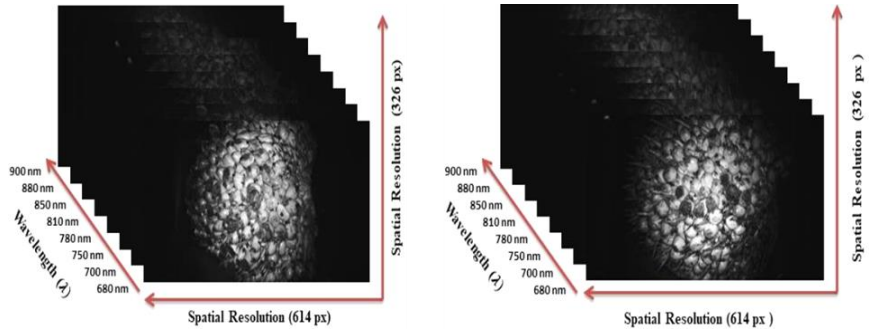

Figure 6. Multispectral data cube of oil palm FFB samples; (a) unripe and (b) ripe

Figure 7 shows the relation of reflectance intensities to wavelength and chemical content of oil palm FFBs. Figure 7(a) represents the average relative reflectance intensities for each ripeness level versus LED wavelengths. Each FFB has 16 images that come from 2 sides and eight wavelengths. It means that each FFB side has eight scannings using different wavelengths. Since there are 15 ripe FFBs, a black data point represents the average relative intensities of 15 FFBs at each LED wavelength. It also applies to grey data points of unripe FFBs. The resulting reflectance intensities of ripe oil palm FFBs are 7.75% higher than the unripe reflectance intensities for each wavelength. The higher intensities of ripe FFB could be due to increasing OC in the mesocarp at the ripe stage and less chlorophyll content [24], [28]. The resulting reflectance intensities increase significantly at 750-900 nm (IR region) except at 780 nm and 880 nm. In other words, IR light is less absorbed by the chemical contents of oil palm mesocarps [24]. Increasing reflectance intensities in IR regions happened for the rapid detection of RFS in rice seed using LED-based multispectral imaging [7]. LEDs at wavelengths of 780 nm and 880 nm have full-width-half-maximum (FWHM) of 40 nm and 50 nm, but the optical powers of both LEDs are 45 mW, higher than other LEDs used. The decreased reflectance intensities at the wavelengths could be due to wide FWHM, which overlaps with adjacent LED wavelengths [6].

OC and FFA are the internal qualities of oil palm FFBs, which are related to the ripeness stage [24]. For ripeness stage validation, we measured the OC and FFA of 30 FFBs using the Soxhlet extraction method, which consisted of 15 unripe and 15 ripe oil palm FFBs. Figure 7(b) shows the OC distribution for the ripeness stages. The graph is displayed based on sample numbers labeled as (S1-S15) for ripe FFBs and (S16-S30) for unripe FFBs. It shows that the OC of ripe FFBs are higher than the unripe FFBs. The ripe FFBs have 16-28% of OC, while the unripe FFBs have 0.5-15%. The OC of oil palm FFB can vary from 1.25% to 53.91% during the ripening stage [21]. The OC measurement shows the influence of the ripeness stages on reflectance intensities, as shown in Figure 7(a). Figure 7(c) shows the FFA content for 30 oil palm samples. The FFA values of the 30 oil palm FFB samples are roughly equal, with a range of 3.81-11.02% for ripe FFBs and 1.83-10.5% for unripe FFBs. However, the average FFA content is somewhat higher for ripe FFBs [24]. The FFA measured in this study is slightly higher than the standard (5%). It could be due to many causes, such as taking a long time between harvesting, scanning, and the Soxhlet extraction process.

3.2. Training and testing results of you only look once version 4 model

The training stage aims to train a machine or deep learning model algorithm on a dataset that consists of annotated images. In this study, we use pre-trained weight YOLOv4 tiny using transfer learning to obtain a robust detection model. Two parameters, mAP and average loss, describe the training results, displayed in a loss function graph as shown in Figure 8. The red line represents the mAP values, while the blue line shows the loss function values. Both values are inversely proportional. Figure 8 shows mAP values increase as the iteration number increases during the training process, attaining 94% at the 1000th iteration and reaching 99.7% at the 6000th iteration. The highest mAP is the highest accuracy that the model can obtain. The loss curve reaches the minimum value at the 6000th iteration with an average loss of 0.0479. The graph shows that the ripeness detection model resulted in the best performance with the highest accuracy of 99.7%.

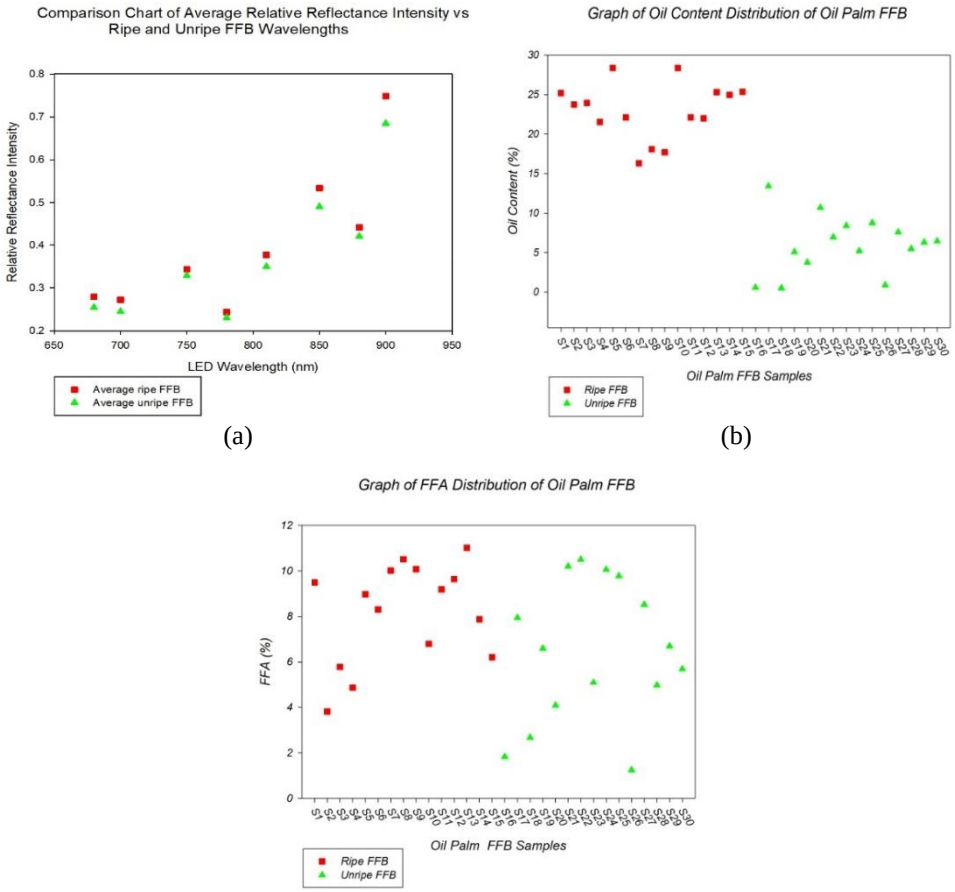

Figure 7. Multispectral imaging results; (a) relative reflectance intensities, (b) OC, and (c) FFA content

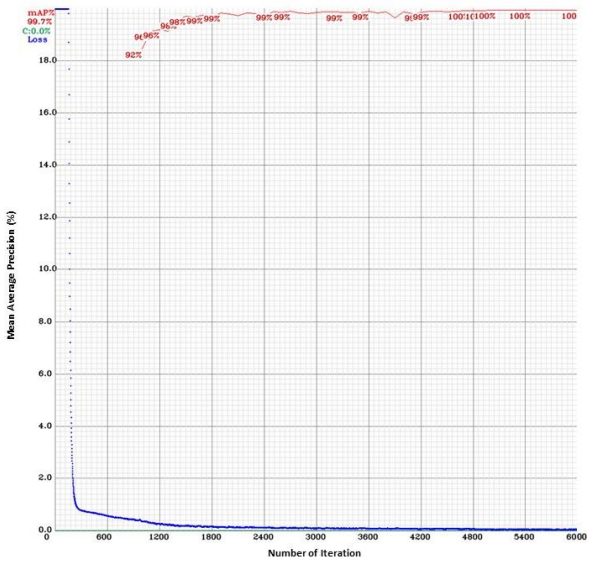

Figure 8. Training results of the loss function

Testing performance evaluation used metric parameters including mAP at IoU values. Table 2 shows the testing results for the two-class YOLOv4 model, on which the testing dataset has 380 images (20% of 1900 images). Each model class, ripe and unripe, has balanced 190 images for the testing stage. The results show the values of mAP @50% and mAp @75% above 75%, which means the model has detected the

ripeness levels of ripe and unripe oil palm FFBs with a confidence threshold above 75%. The AP results in Table 2 range from 99.4–99.6%. The testing results also display the model performance in terms of TP, FP, and FN, where the FP and FN numbers are far less than TP values, resulting in higher accuracy. Precision and recall reach values higher than 95%. Higher FP could be because of different image textures between front and back side FFBs included in the datasets. The performance parameters for the unripe level are lower than the ripe level, especially the precision value of 0.88, related to a higher FP of 26 than the ripe level.

Table 2. Metrics results for still images dataset splits for YOLO model testing

Parameters	Ripe	Unripe
Class	Ripe	Unripe
Confusion matrix	[[189, 17], [1, 0]]	[[188, 26], [1, 0]]
TP	189	188
FP	17	26
FN	1	2
Precision	0.92	0.88
Recall	0.99	0.99
F1-score	0.95	0.93
AP	99.55%	99.40%
mAP (@0.50)	99.47%	
mAP (@0.70)	81.01%	

The testing results are comparable to other YOLOv4 models. The results agree with the case for on–tree oil palm FFBs using a USB color camera, which resulted in the mAP of 87.9% [21]. In addition, our results are also comparable to using the YOLOv4 models for stacked oil palm FFBs with six-class ripeness levels. It obtained mAP @50% of 99.89 for the testing stage, about 0.4% higher than the results in Table 2 [23]. The experiment used a large dataset of about 3000 images of unripe and ripe oil palm FFBs in RGB color space. It showed that multispectral images with monochrome images and the YOLOv4 algorithm obtained similar and somewhat higher accuracy as the RGB color images [29]. The use of multispectral images has more advantages due to being less sensitive to background light [14] and being able to do classification, chemometrics, and object detection at the same time, such as detecting foreign objects on chili peppers using hyperspectral imaging and the YOLOv5 algorithm, which obtained a recognition rate of over 96% with the shortest detection time of approximately 12 ms [30].

3.3. You only look once version 4 model validation results

Validation of the YOLO model in this study used two ways, with 100 still images and video of 30 oil palm FFBs. Figure 9(a) shows the validation result for still images recorded during dataset acquisition with each oil palm FFB sitting in the middle of the multispectral system (optical box). The bounding box of each class has a blue color for ripe and a green color for unripe class. Figure 9(a) shows the higher to lower detection or recognition accuracy from left to right. The detection accuracies are 0.98, 0.86, and 0.49 for ripe images (Figure 9(a) point (a)-(c)). The accuracy of 49% means the ripe FFB is still recognizable as ripe, but the image intensity is the same as the unripe class. The bottom figure is for unripe oil palm FFB images (Figure 9(a) point (d)-(f)), which have accuracy from left to right as 0.95, 0.83, and 0.74. The accuracy of 0.74 shows the image is brighter than the other unripe image, which is most likely caused by the basal part of FFBs having brighter colors than the middle part. The unripe class detection accuracies vary only slightly due to less variety in blackish colors. The ripe class model has more accuracy variation, possibly caused by the color variety of ripe oil palm FFBs, which include under-ripe, ripe, and overripe FFBs [22]. Other causes of accuracy discrepancy were observed due to the variety of oil palm FFB sizes at the same class while the ripeness level is the same and illuminating light. They could affect the non-maximum suppression (NMS) threshold. Inconsistency in the labeling process could also influence the IoU [19], [23]. Table 3 shows the validation performance metrics of still FFBs and moving FFBs on the conveyor. The left part of Table 3 shows the validation results for 49 ripe and 51 unripe still oil palm FFB images. The validation stage obtained mAP of 99.55% for ripe and 99.4% for unripe class with mAP (@0.50) of 98.60% and mAP (@0.70) of 81.71%.

The validation process also used video recording of 30 oil palm FFBs (15 ripe and 15 unripe FFBs) for real-time testing. The videos utilized a monochrome camera and LED-based multispectral imaging of continuous oil palm FFBs on a moving conveyor. The conveyor has buckets made on two plates on the conveyor floor, each bucket filled with an oil palm bunch. In the video recording, all LEDs were on. Figure 9(b) shows some video frames with the accuracy and class name on each bounding box (red for "matang" or ripe) and (blue for "mentah" or unripe). The TP condition is feasible in Figure 9(b) point (a), where the actual value is ripe as the model detects it as ripe. The FP situation is shown in Figure 9(b) point (b), where the sample was unripe, but the model predicted it as ripe. The FN was seen in Figure 9(b) point (c), where the actual sample was ripe but predicted unripe. The FP and FN conditions are known as overfitting, in which the model performance

is better during training but worse during testing and validation, especially using video of moving oil palm FFBs. The cause could be an inhomogeneous LED light incident on the FFB top surface reflected by the conveyor plate. The improvements in light intensity and camera specifications can overcome lower recognition accuracy [31]. Table 3 right shows the model validation metrics using videos of moving oil palm FFBs. It shows the ability of the model to detect with an AP of 99.69% for ripe and 99.62% for unripe, with IoU of 79.59% and mAP (@0.50) of 99.66%. The model has an FPS range of 2.99-3.88, and the average duration time per FFB was 2 seconds. The result was comparable with the experiment using videos of stacked oil palm FFBs on the concrete ground using a smartphone camera [29].

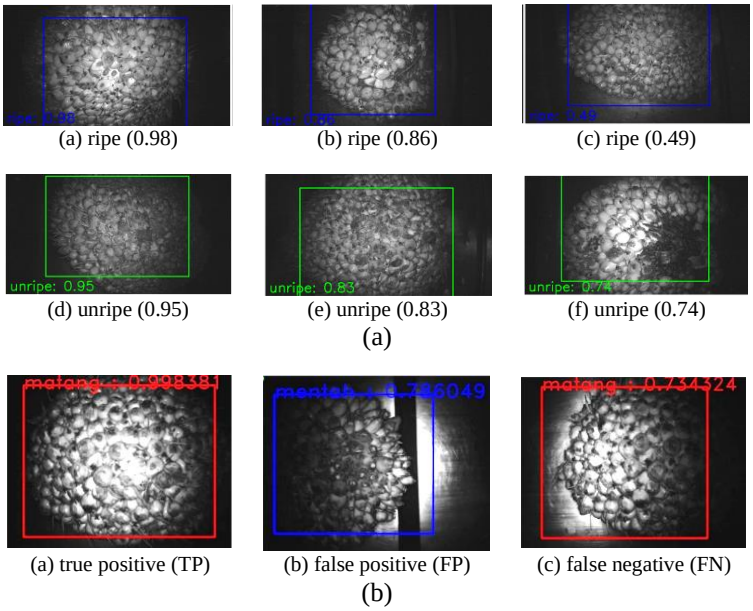

(a) ripe (0.98) (b) ripe (0.86) (c) ripe (0.49)
(d) unripe (0.95) (e) unripe (0.83) (f) unripe (0.74)
(a)
(a) true positive (TP) (b) false positive (FP) (c) false negative (FN)
(b)

Figure 9. Results of YOLOv4 tiny model validation on oil palm images, ripe (blue) and unripe (green) using; (a) still images and (b) videos

Table 3. Metrics for validation results of still oil palm images and video frames

	Still images		Video frames	
Parameters	Ripe	Unripe	Ripe	Unripe
Class	ripe	unripe	ripe	unripe
Confusion matrix	[[49, 5], [0, 0]]	[[49, 6], [2, 0]]		
TP	49	49	12	11
FP	5	6	3	4
FN	0	2	2	2
Precision	0.91	0.89	0.8	0.73
Recall	1.00	0.96	0.85	0.84
F1-score	0.95	0.92	0.82	0.78
AP	99.55%	99.4%	99.69%	99.62%
mAP (@0.50)	98.60%		99.66%	
mAP (@0.70)	81.71%			
Duration			2 Second	

4. CONCLUSION

This study has shown the ability of an LED multispectral system and deep learning of the YOLOv4 algorithm to detect the ripeness of oil palm FFBs. The reflectance intensity measurement was capable of showing the difference between ripe and unripe oil palm FFBs. The OC and FFA were able to differentiate the ripeness levels. The results show higher values of OC and slightly higher values of FFA for ripe FFBs, which are related to higher relative reflectance intensities. The YOLO detection model has four tasks: training, testing, evaluation using still images, and evaluation using video of oil palm FFBs on a moving conveyor. There were 2000 images for the training, testing, and validation process. The training stage resulted in a mAP of 99.7% and an average loss of 0.0479. The testing stage obtained mAP above 95% for both ripeness levels. The evaluation using 100 still images and videos for each level showed that the precision, recall, and F1 scores were less for the unripe level and decreased for video than for still image

validation. Our future works include using YOLO algorithms to detect defective oil palm FFBs and to classify ripeness levels using an improved LED-based multispectral system and ANN in our sorting and grading MV, applied for sorting areas in palm oil mills.

ACKNOWLEDGEMENTS

The authors would like to acknowledge DRTPM, Universitas Riau Institute of Research and Community Service (LPPM) and PTPN V Indonesia for supporting this study. This study was funded by DRTPM under Research Grant with contract number of 157/E5/PG.02.00.PL/2023.

REFERENCES

[1] A. Hussain, H. Pu, and D. W. Sun, "Innovative nondestructive imaging techniques for ripening and maturity of fruits – A review of recent applications," *Trends in Food Science and Technology*, vol. 72, pp. 144-152, 2018, doi: 10.1016/j.tifs.2017.12.010.

[2] H. Cakmak, "Assessment of fresh fruit and vegetable quality with non-destructive methods," *Food Quality and Shelf Life*, pp. 303-331, 2019, doi: 10.1016/B978-0-12-817190-5.00010-0.

[3] J. A. Fracarolli, F. F. A. Pavarin, W. Castro, and J. Blasco, "Computer vision applied to food and agricultural products," *Engenharia Agrícola*, vol. 51, no. 5, 2020, doi: 10.5935/1806-6690.20200087.

[4] L. Kaiyan, L. Chang, S. Huiping, W. Junhui, and C. Jie, "Review on the Application of Machine Vision Algorithms in Fruit Grading Systems," *Advances in Intelligent Systems and Computing*, vol. 1304, pp. 271–280, 2021, doi: 10.1007/978-3-030-63784-2_34.

[5] A. Ibrahim *et al*., "Preliminary Study for Inspecting Moisture Content, Dry Matter Content, and Firmness Parameters of Two Date Cultivars Using an NIR Hyperspectral Imaging System," *Frontiers in Bioengineering and Biotechnology*, vol. 9, p. 720630, 2021, doi: 10.3389/fbioe.2021.720630.

[6] M. A. T. Monsalve, G. Osorio, N. L. Montes, S. Lopez, S. Cubero and J. Blasco, "Characterization of a Multispectral Imaging System Based on Narrow Bandwidth Power LEDs," in *IEEE Transactions on Instrumentation and Measurement*, vol. 70, pp. 1-11, 2021, doi: 10.1109/TIM.2020.3010109

][7] H. Weng *et al*., "Development of a low-cost narrow band multispectral imaging system coupled with chemometric analysis for rapid detection of rice false smut in rice seed," *Sensors*, vol. 20, no. 4, p. 1209, 2020, doi: 10.3390/s20041209.

[8] C. Ma, M. Yu, F. Chen, and H. Lin, "An Efficient and Portable LED Multispectral Imaging System and Its Application to Human Tongue Detection," *Applied Sciences*, vol. 12, no. 7, p. 3552, 2022, doi: 10.3390/app12073552.

[9] S. Gaikwad and S. Tidke, "Multi-Spectral Imaging for Fruits and Vegetables," *International Journal of Advanced Computer Science and Applications (IJACSA)*, vol. 13, no. 2, pp. 743-760, 2022, doi: 10.14569/IJACSA.2022.0130287.

[10]. J. Du, "Understanding of Object Detection Based on CNN Family and YOLO," *Journal of Physics: Conference Series*, 2018, vol. 1004, no. 1, doi: 10.1088/1742-6596/1004/1/012029.

[11] L. Huang, R. Luo, X. Liu, and X. Hao, "Spectral imaging with deep learning," *Light: Science and Applications*, vol. 11, no. 1, p.61, 2022, doi: 10.1038/s41377-022-00743-6.

[12] J. Xu and P. Mishra, "Combining deep learning with chemometrics when it is really needed: A case of real time object detection and spectral model application for spectral image processing," *Analytica Chimica Acta*, vol. 1202, p. 339668, 2022, doi: 10.1016/j.aca.2022.339668.

[13] S. Li, Y. Li, Y. Li, M. Li, and X. Xu, "YOLO-FIRI: Improved YOLOv5 for Infrared Image Object Detection," *IEEE Access*, vol. 9, pp. 141861–141875, 2021, doi: 10.1109/ACCESS.2021.3120870.

[14] S. Bhowmick, S. Kuiry, A. Das, N. Das, and M. Nasipuri, "Deep Learning-Based Outdoor Object Detection Using Visible and Near-Infrared Spectrum," *Multimedia Tools and Applications*, vol. 81, pp. 9385–9402, 2022, doi: 10.1007/s11042-021-11848-2.

[15] W. Lai, M. Zhou, F. Hu, K. Bian, and H. Song, "Coal Gangue Detection Based on Multi-Spectral Imaging and Improved YOLO v4," *Acta Optica Sinica*, vol. 40, no. 24, p. 2411001, 2020, doi: 10.3788/AOS202040.2411001.

[16] L. S. Woittiez *et al.*, "Smallholder Oil Palm Handbook Module 2: Harvesting, Grading, Transport," 3rd ed., vol. 2. SNV *International Development Organisation and Wageningen University*. 2016.

[17] C. H. Lim, V. L. K. Loo, S. L. Ngan, B. S. How, W. P. Q. Ng, and H. L. Lam, "Optimisation of industry revolution 4.0 implementation strategy for palm oil industry in cyber security," *Chemical Engineering Transactions*, vol. 81, pp. 253-258, 2020, doi: 10.3303/CET2081043.

[18] M. Shiddiq, H. Herman, D. S. Arief, E. Fitra, I. R. Husein, and S. A. Ningsih, "Wavelength selection of multispectral imaging for oil palm fresh fruit ripeness classification," *Applied Optics*, vol. 61, no. 17, pp. 5289-5298, 2022, doi: 10.1364/ao.450384.

[19] N. A. M. B. Selvam, Z. Ahmad and I. A. Mohtar, "Real Time Ripe Palm Oil Bunch Detection using YOLO V3 Algorithm," *2021 IEEE 19th Student Conference on Research and Development (SCOReD)*, Kota Kinabalu, Malaysia, 2021, pp. 323-328, doi: 10.1109/SCOReD53546.2021.9652752.

[20] M. H. Junos, A. S. M. Khairuddin, S. Thannirmalai, and M. Dahari, "An optimized YOLO-based object detection model for crop harvesting system," in *IET Image Process*, vol. 15, no. 9, pp. 2112–2125, Jul. 2021, doi: 10.1049/ipr2.12181.

[21] J. W. Lai, H. R. Ramli, L. I. Ismail, and W. Z. W. Hasan, "Real-Time Detection of Ripe Oil Palm Fresh Fruit Bunch Based on YOLOv4," in *IEEE Access*, vol. 10, pp. 95763–95770, 2022, doi: 10.1109/ACCESS.2022.3204762.

[22] M. Y. M. A. Mansour, K. D. Dambul, and K. Y. Choo, "Object Detection Algorithms for Ripeness Classification of Oil Palm Fresh Fruit Bunch," *International Journal of Technology (IJTech)*, vol. 13, no. 6, p. 1326, Nov. 2022, doi: 10.14716/ijtech.v13i6.5932.

[23] Suharjito, M. Asrol, D. N. Utama, F. A. Junior, and Muhaimin "Real-Time Oil Palm Fruit Grading System Using Smartphone and Modified YOLOv4," in *IEEE Access*, vol. 11, pp. 59758-59773, 2023, doi: 10.1109/ACCESS.2023.3285537.

[24] M. Shiddiq *et al*., "Oil Content and Free Fatty Acid Prediction of Oil Palm Fresh Fruit Bunches Using Multispectral Imaging and Partial Least Square Algorithm," *N. I. Inda et al. (Eds.): ISST* pp. 143–154, 2023, doi: 10.2991/978-94-6463-228-6_17

[25] Z. Iqbal, S. Herodian, and S. Widodo, "Development of Partial Least Square (PLS) Prediction Model to Measure the Ripeness of Oil Palm Fresh Fruit Bunch (FFB) by Using NIR Spectroscopy," in *IOP Conference Series: Earth and Environmental Science*, Manila, 2019, vol. 347, p. 012079, doi:10.1088/1755-1315/347/1/012079.

[26] A. I. B. Parico and T. Ahamed, "Real time pear fruit detection and counting using yolov4 models and deep sort," in *Sensors*, vol. 21, no. 14, p. 4803, 2021, doi: 10.3390/s21144803.

[27] M. O. Lawal, "Tomato detection based on modified YOLOv3 framework," *Scientific Reports*, vol. 11, p. 1447, Jan. 2021, doi: 10.1038/s41598-021-81216-5
[28] J. W. Lai, H. R. Ramli, L. I. Ismail, W. Z. W. Hasan, "Oil Palm Fresh Fruit Bunch Ripeness Detection Methods: A Systematic Review," *Agriculture*, vol. 13, no. 1, p. 156, 2023, doi: 10.3390/agriculture13010156.
[29] F. Suharjito *et al*., "Annotated Datasets of Oil Palm Fruit Bunch Piles for Ripeness Grading Using Deep Learning," *Data Descriptors*, vol. 10, no. 1, p. 72, 2023, doi: 10.1038/s41597-023-01958-x.
[30] Z. Shu, X. Li, and Y. Liu, "Detection of Chili Foreign Objects Using Hyperspectral Imaging Combined with Chemometric and Target Detection Algorithms," in *Foods*, vol. 12, no. 13, p. 2618, 2023, doi: 10.3390/foods12132618.
[31] M. A. Genaev *et al*., "Classification of Fruit Flies by Gender in Images Using Smartphones and the YOLOv4-Tiny Neural Network," *Mathematics*, vol. 10, no. 3, p. 295, 2022, doi: 10.3390/math10030295.

BIOGRAPHIES OF AUTHORS

Minarni Shiddiq is a full professor at Department of Physics, Faculty of Mathematics and Science, University of Riau. Her current research interests include optoelectronic systems, hyperspectral and multispectral imaging, computer vision, and machine vision, and laser applications. She is currently working in implementing hyperspectral and multispectral imaging in sorting and grading oil palm fresh fruits and plastics sortation. She can be contacted at email: minarni.shiddiq@lecturer.unri.ac.id.

Saktioto is a full professor at Department of Physics, Faculty of Mathematics and Science, University of Riau. He works on Plasma and Photonics Physics. He has published many articles and supervised master and doctoral degree since 2009. His current research interests include the field of photonics, plasma, and its applications such as fiber optics and microwave plasma as communication, medical, and industrial technologies. He can be contacted at email: saktioto@lecturer.unri.ac.id.

Roni Salambue is a lecturer at Department of Informatics, Faculty of Mathematics and Science, University of Riau. His current research interests include creating model machine learning, and especially computer vision. He can be contacted at email: roni.salambue@lecturer.unri.ac.id.

Fiqra Wardana was a student at University of Riau 2018 and has finished studying Information System with a B.Sc. degree in 2022. His research interests include creating model machine learning especially computer vision. Detecting oil palm fruit using Tensorflow model and implementing it using camera android. He can be contacted at email: fiqra22@gmail.com.

Vicky Vernando Dasta B.Sc. in Physics from University of Riau. Research area includes applied computer vision in agriculture. Currently working on machine vision research for sortation of palm fruit bunch at Laboratory of Photonics at University of Riau. He can be contacted at email: vickydasta@gmail.com.

Ihsan Okta Harmailil was a student at University of Riau 2019 and has finished studying Physics at Department of Physics, Universitas Riau with a B.Sc. degree in 2023. His research interests include multispectral imaging and object detection. He is now continuing Master's degree at Universiti Kebangsaan Malaysia. He can be contacted at email: oktaihsan02@gmail.com.

Mohammad Fisal Rabin was a student at University of Riau 2014 and has finished studying Physics at Department of Physics, Universitas Riau with a B.Sc. degree in 2019. His research interests include hyperspectral imaging and automation. He has just graduated for his M.Sc. from the same Department of Physics and working in building a LED based multispectral imaging for oil palm FFB ripeness detection. He can be contacted at email: fisal.rabin25@gmail.com.

Nisa Arpyanti was a student at University of Riau 2017 and has finished studying Physics at Department of Physics, Universitas Riau with a B.Sc. degree in 2022. His research interests include multispectral imaging and object detection. She is now continuing Master's degree at Riau University. She can be contacted at email: nisaarpyanti@gmail.com.

Dilham Wahyudi was a student at University of Riau 2018 and has finished studying Physics at Department of Physics, Universitas Riau with B.Sc. degree in 2023. His research interests include imaging, artificial intelligence, and automation. He can be contacted at email: dilhamwahyudi11@gmail.com.